Composites Part B 90 (2016) 523–529

Contents lists available at ScienceDirect

Composites Part B

journal homepage: www.elsevier.com/locate/compositesb

Damage accumulation in a carbon fiber fabric reinforced cyanate ester composite subjected to mechanical loading and thermal cycling

Jihane Ajaja, François Barthelat*

Mechanical Engineering Department, McGill University, Canada

ARTICLE INFO

Article history:
Received 12 December 2014
Received in revised form
22 September 2015
Accepted 23 September 2015
Available online 28 October 2015

Keywords:
A. Fabrics
A. Carbon fibre
A. Theromosetting resin
D. Mechanical testing
D. Optical microscopy

ABSTRACT

Carbon fiber reinforced cyanate ester composites are of interest for space structural applications because of their high specific strength and stiffness, but also for their dimensional stability and resistance to microcracking. This new type of composite materials is promising, but so far experimental data remains scarce. In this work we have characterized the microcracking behavior of a cyanate ester composite, focusing on the conditions under which microcracking initiates. The performance of these composites for space applications was investigated by focusing on the accumulation of damage from extreme thermal and externally applied stresses. For this purpose, a five-harness satin weave in $[0/45]_s$ was subjected to micromechanical testing in three point bending. Microdamage accumulating during monotonic loading was monitored by in-situ imaging, and we also show that cyclic tests of increasing amplitude can detect such damage. We also subjected the material to cyclic thermal stress using thermomechanical and dynamic mechanical analyzers (TMA and DMA) and a fast thermal cycling method. For these tests, no variation in the coefficient of thermal expansion (CTE) or degradation in modulus from thermal cycling under TMA and DMA, and no microcracking could be detected from visual inspection. However, faster thermal cycling resulted in the formation of microcracking and a significant reduction in modulus. These results suggest a possible failure mode for this type of material, which should be taken into consideration for aerospace applications.

© 2015 Elsevier Ltd. All rights reserved.

1. Introduction

Carbon fiber reinforced composite materials have drawn particular attention during the past decades for their remarkable thermal [1,2], electrical [1] and mechanical properties [1–9], making these excellent choices for high performance applications including but not restricted to, satellites, space vehicles, cryogenic tanks, aircrafts and helicopters [2,3,6–8,10–20]. For some of these applications, the operating conditions are considered extreme. For example artificial satellites, as they enter and exit earth's shade, endure high amplitude thermal cycles. In the earth's shadow, the satellite cools down and reaches a temperature of −160 °C, and heats up to +130 °C when it is exposed to direct sun light, representing thermal cycles with amplitudes exceeding 300 °C. The composite materials used in the structure of these satellites therefore undergo extreme temperature cycles which may induce microdamage or even catastrophic failure. Several authors have characterized damage accumulation in composites, for example by measuring the density of microcracks as function of number of thermal cycles [3,21–24]. Others have assessed the accumulation of damage from external loading and thermal cycling through the monitoring of the Young's modulus. Ahlborn [11] assessed the degradation in modulus as a function of increasing number of cycles in a carbon fiber reinforced PEEK composite in $[0]_{18}$. Boccaccini et al. and Bonara et al. [25] both developed models allowing to determine the drop in modulus induced by damage based on initial physical and mechanical properties and Schubbe et al. [19] studied the effect of damage accumulation on a 5-harness woven composite in order to assess its effects on the variation of mechanical properties based on the degradation in Young's modulus and so did Rivera et al. [26] on a carbon fiber reinforced vinylester composite. This study intends to characterize the microcracking behavior of a carbon fiber reinforced cyanate ester composite resulting from the application of extreme thermal and externally applied stresses.

* Corresponding author.
E-mail address: francois.barthelat@mcgill.ca (F. Barthelat).

http://dx.doi.org/10.1016/j.compositesb.2015.09.054
1359-8368/© 2015 Elsevier Ltd. All rights reserved.

2. Material preparation

Five-harness satin weave laminates in $[0/45]_s$ were produced from commercially available EX-1515 prepregs (TENCATE, California, USA) consisting of a cyanate ester polymeric matrix and selected YSH-50A-10S pitch fibers (Nippon Graphite Fiber Corporation, Tokyo, Japan) as seen on Fig. 1. Prepregs were cured at 121 °C resulting in a fiber volume of 60 ± 5% and a maximum void content of 2.0% per volume. No post-curing treatment was carried out. All specimens were provided by Composite Atlantic Limited (Mirabel, Canada) and consisted of four-ply symmetric laminates, each ply having a thickness of 0.46 ± 0.05 mm. For imaging purposes, the samples were grinded using sand papers between 320 and 1200 grit, followed by polishing using 6 μm followed by 1 μm suspension particles. An upright optical microscope was used to image the samples at varying magnifications before, during and after testing.

3. Monotonic tests

In order to assess the basic properties of the laminate as well as its failure modes, bending tests were performed on small beams of 3.5 mm by 15.0 mm by 0.5 mm cut from the laminate using a high-precision diamond saw. The side of the sample was polished following the procedure described above, and the sample was then placed in a three-point bending fixture mounted on a miniature loading stage (E. Fullam, NY) equipped with a 445 N load cell. The loading stage was then placed under an upright optical microscope (Olympus, Richmond Hill) equipped with a CCD camera (QImaging, Surrey) for in-situ imaging during the test. During the test, the sample was loaded monotonically at a rate of 0.5 μm/s until total failure of the sample (i.e. until the force dropped to zero). Flexural stresses and strains were computed from the force and displacement, using standard beam theory [28]. Fig. 2 shows a typical stress–strain curve for this material, together with a series of images taken during the test. Initially the material is linear elastic with a flexural modulus of 150 GPa. At a stress of about 600 MPa the material deviated from the linear trend and softened, but the stress kept increasing up to a stress of 900 MPa (strain = 15%). Past the maximum stress, the material softened rapidly to total failure. The in-situ images were used to track the failure mode(s) in this material. The first image (Fig. 2 a)) shows the undamaged state of the material before the test is initiated at (0,0) (strain, stress (MPa)). No microcracking could be observed in the linear elastic region, and in the region immediately after the first softening at 600 MPa. Softening was therefore attributed to yielding of the matrix. A first crack appeared at a stress of 873 MPa (0.011 strain), as shown on Fig. 2 b). The crack formed in the outer ply of the laminate on the compression side, close to where the load is applied. As the test progressed, this crack further propagated into the interlaminar region. At the same time, delamination cracks appeared in the inner plies (Fig. 2 c)). Further increasing the strain resulted in further crack propagation from the outer ply across into the inner plies (Fig. 2 d)) and subsequently to total failure of the material (Fig. 2 e)). The overall picture of the fractured material is shown on Fig. 3. The region circled in red refers to the region imaged during the test and corresponds to the crack initiation site on the composite laminate. This image shows that damage initiates from microbuckling at the outer ply of the laminate and evolves in the form of delamination. Karger-Kocsis et al. [29] reported similar observations, with microbuckling occurring due to the 3D nature of the reinforcement. As the outer ply initially cracks, the applied load is transferred to the inner plies until the crack propagates between the inner plies leading to the material's failure. The exact sequence of the failure events is function of the interfacial characteristics between the matrix and the fibers.

4. Damage accumulation in flexion

Imaging during the monotonic test revealed a progressive accumulation of microcracking and damage once the material was loaded beyond a critical stress of about 800 MPa. The in-situ imaging we used in the previous section requires polishing and optical microscopy, which might not be possible on larger samples with complex geometries. In addition, the method only reveals cracks which emerge on the polished surface, other cracks may develop within the material and remain undetected with this method. In this section the prospect of quantitatively monitoring damage accumulation without the need for in-situ imaging is explored. In order to assess damage accumulation in the material, cyclic three point bending tests have been carried out. Those were achieved by increasing the amplitude of the strain as the test progressed, until reaching failure of the material (Fig. 4).

A typical stress–strain curve resulting from this test is shown on Fig. 5. The stress strain alternate from a maximum stress to a stress close to zero, each cycle taking the material closer to failure.

The envelope of this cyclic stress–strain curve is similar to the monotonic stress–strain curve presented in the previous section, but in this case, the instantaneous modulus of the material can be determined using the linear loading and unloading segments. In turn, the modulus was used to assess damage in the material using a simple damage model [6,30–33] where D represents the damage variable, E the instantaneous modulus and E_0 the undamaged modulus:

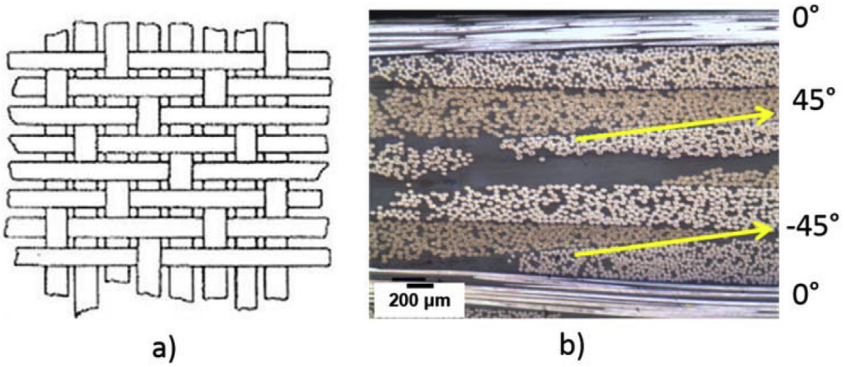

Fig. 1. a) 3D view of a 5-harness satin weave composite [27] b) cross-section view of laminate.

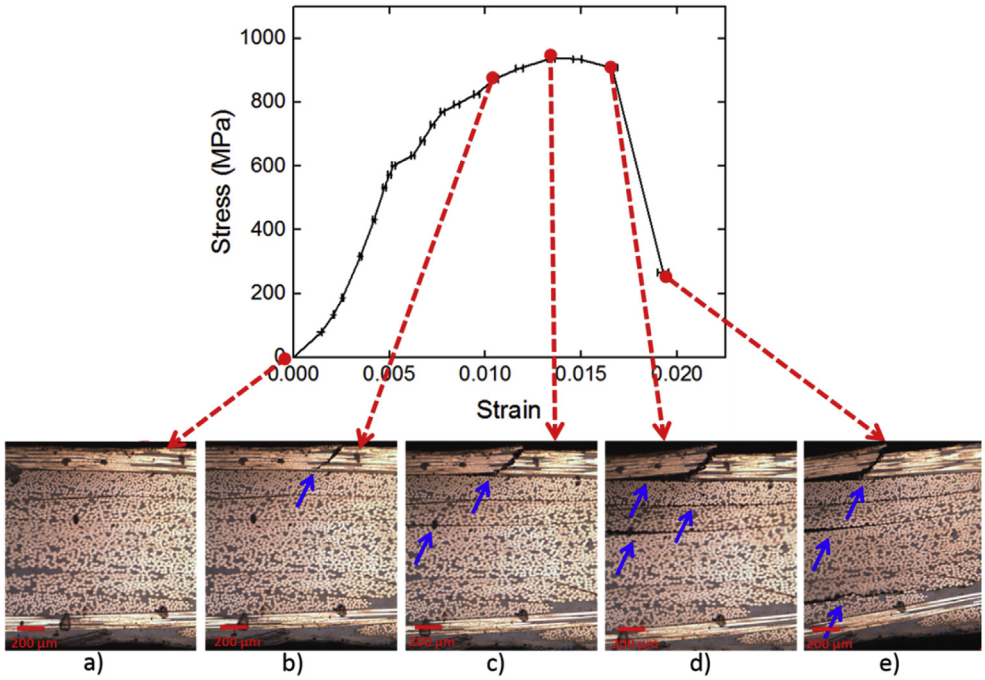

Fig. 2. Typical flexural stress–strain curve for the laminate, combined with images of the surface acquired during the test.

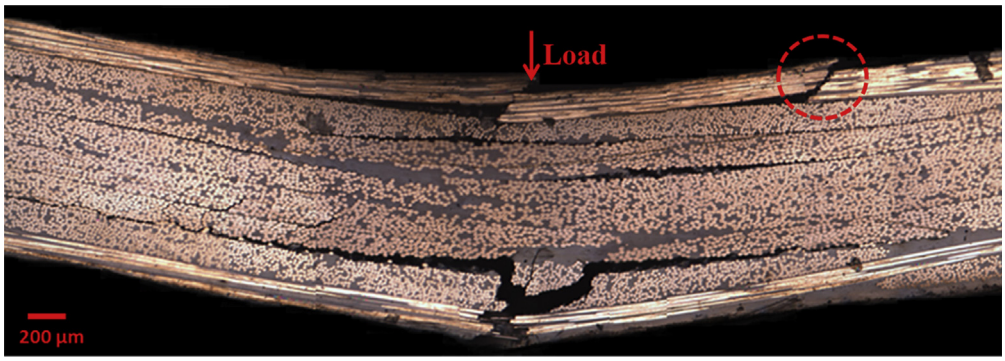

Fig. 3. Overall picture of the fractured laminate.

$$D = 1 - \frac{E}{E_0} \quad (1)$$

In the simple damage model, $D = 0$ corresponds to the intact material ($E = E_0$) while $D = 1$ corresponds to a fully damaged material ($E = 0$). In reality, catastrophic failure occurs at a critical damage variable $D_c < 1$. Fig. 6 shows the combined results for a series of different tests performed on seven different samples. These curves show that damage accumulate, on average, a strain of about 0.0085, which corresponds to a stress of about 580 MPa using the stress–strain curve. This result shows that microcracking in fact commences as soon as the stress–strain curve deviates from a linear behavior (Fig. 2). Past this threshold, the modulus decreases continuously and damage accumulated with increasing applied strain until the materials reached failure.

Similarly to monotonic tests, the crack initiation site for cyclic tests occurred on the outer ply of the material, on the compression side corresponding to microbuckling as shown on Fig. 7. Microbuckling also leads to delamination with increasing number of cycles as crack propagation and growth occurs.

5. Damage from slow thermal cycling

In the previous sections, microdamage was generated in the material by applying an external mechanical load. In this section,

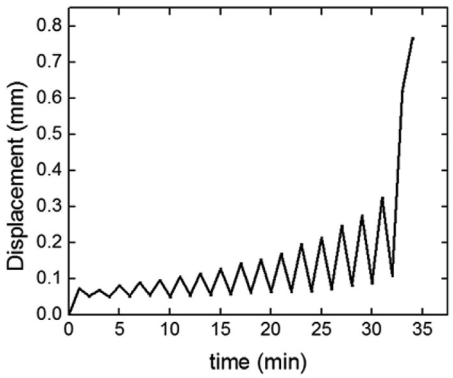

Fig. 4. Increasing displacement vs. time.

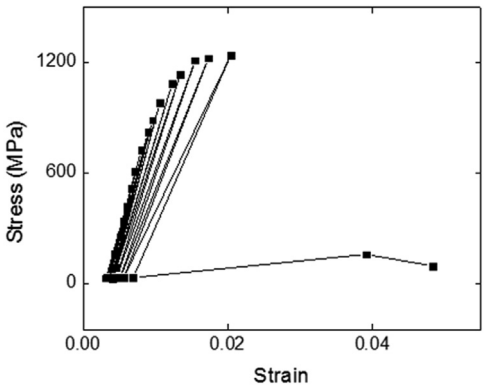

Fig. 5. Stress-strain curve obtained from a cyclic three point bending test.

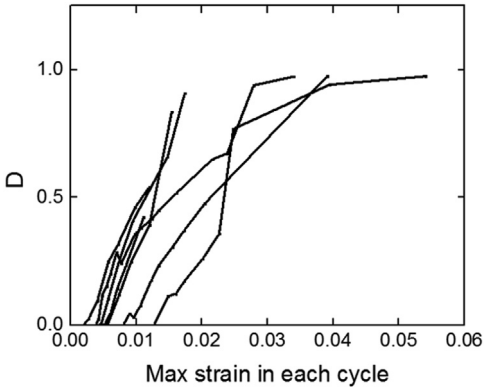

Fig. 6. Damage variable as a function of maximum strain in each cycle.

we investigate how internal stresses generated by thermal effects (i.e. mismatch of thermo-elastic properties between matrix and fibers) can generate damage. In a first series of tests, the coefficient of thermal expansion (CTE) was measured using a thermo-mechanical analysis (TMA Q400, TA Instruments) on 0.5 mm thickness samples. Those samples were subjected to a number of thermal cycles with temperatures varying from −70 °C to 150 °C. The dimensional change in the material with respect to temperature was monitored and allowed to track any change in the material's coefficient of thermal expansion (CTE). As shown on Fig. 8, no change in CTE was observed after 16 thermal cycles. Those results agree with [34] where no change in CTE with increasing number of thermal cycles was observed for woven composite materials. In the next series of tests, thermal cycles at temperatures varying from 20 °C to −120 °C were imposed on a small sample using a dynamic mechanical analyzer (DMA Q800, TA Instruments). The sample dimensions had a width, length and thickness of 5 mm, 50 mm and 0.5 mm respectively. Over the course of thermal cycling, the samples were subjected to cyclic flexural deformations of small amplitude in a three-point-bending configuration. The amplitude was small enough to ensure that the material remained within elastic limits, but sufficiently large to measure the instantaneous modulus for the material. Modulus values were recorded both at 20 °C and −120 °C to ensure the temperature at which they are recorded does not affect our analysis. The results of this test showed no variation in modulus with increasing number of thermal cycles (Fig. 8 b), indicating that this range of temperature was not sufficient to generate damage in this material.

The absence of microcracks was confirmed by performing various imaging analyses on all tested samples. Images were taken at increasing magnifications reaching 1000X to ensure the absence of microcracks is not due to the difficulty of observing small size cracks. In a similar way, Zhang et al. [35] have reported the absence of microcracks after 50 thermal cycles (−55 to 120 °C) in a braided carbon/epoxy composite. Fig. 9 shows images of a few locations on a representative sample after thermal cycling. All taken images confirm the absence of microcracks on the various studied samples.

6. Damage from fast thermal cycling

As a final test, extreme thermal cycling was applied on samples with varying dimensions corresponding to widths, lengths and thickness of respectively 3.5–25 mm, 20–25 mm and 0.5 mm using a “fast dipping” method, duplicating the condition of a thermal shock where the temperature does not have time to equilibrate, giving rise to temperature and stress gradients within the material. The method consisted in subjecting the samples to a “fast dipping” method, where a series was subjected to cold cycling (20 °C to −210 °C to 20 °C) Samples were dipped in liquid nitrogen (−210 °C) for a period of 10 min and directly transferred to room temperature water (20 °C) for a period of 5 min. This procedure was repeated until ten cycles were completed, which was sufficient to observe damage of some of the samples. After thermal cycling the surface of the samples were imaged using optical microscopy. This procedure revealed that while large regions in the sample remained intact (Fig. 10 a), other regions on the same sample where damaged after three cycles only (Fig. 10 b). In this case cracks appeared in the form of delamination on the outer ply of the composite laminate.

Those images demonstrate that the damage generated by extreme cold cycling for a cyanate ester composite results in delamination from the outer ply but doesn't not propagate to the inner plies, and that no presence of transversal cracks has been observed during the various tests and analyses carried out.

A series of three point bending tests were also carried out on samples before and after five cold tests in order to evaluate the effect of microscopic damage on mechanical properties. These tests revealed an initial modulus of 97.2 ± 1.5 GPa (before thermal cycling) and a modulus of 51.3 ± 6.5 GPa after thermal cycling. This corresponds to a drop of almost 50% in bending stiffness after five cycles only, corresponding to a severe amount of damage (D = 0.5). This result confirmed that instantaneous stiffness of a composite

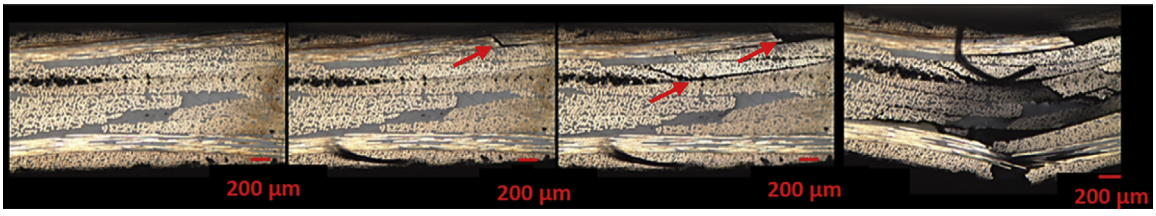

Fig. 7. Damage accumulation under cyclic loading.

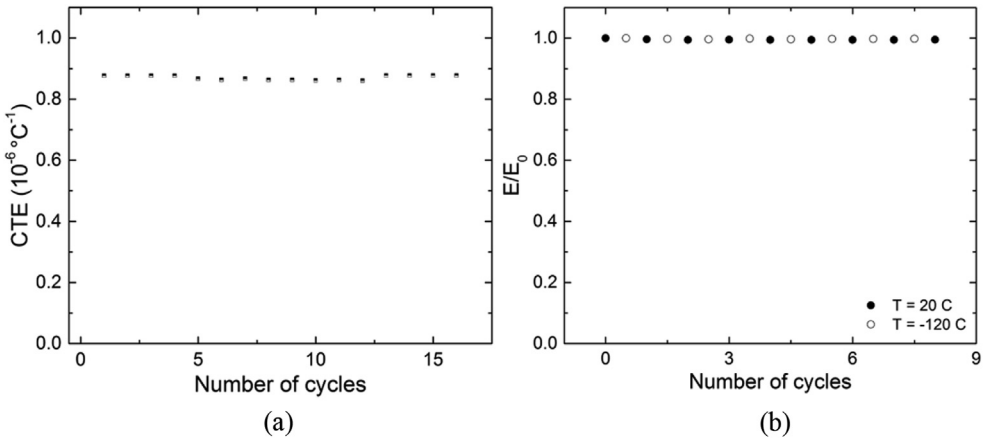

Fig. 8. a) Typical plot of dimensional change vs. temperature obtained from TMA measurements b) Variation in modulus as a function of increasing number of thermal cycles.

structure or material can be used to monitor damage. The stiffness method presents several advantages over imaging: it is faster than imaging, does not require sectioning and polishing of the material, and is non-destructive. We also explored the effect of "hot cycling" on the sample. For these tests, the samples were dipped in boiling water (100 °C) for a period of 10 min and directly transferred to room temperature water (20 °C) for a period of 5 min. This procedure was also repeated until ten hot cycles were completed where different regions in a single sample were imaged in order to track the damage in the entire sample. Fig. 11 a) shows images taken before and after one and 10 cycles in a region on a typical sample. Delamination on the outer ply of the laminate could be observed after only one cycle, and after ten cycles, additional delamination was observed on the other outer ply of the laminate. Fig. 11 b) shows images of another region on the same sample after five and eight cycles. After five cycles, we observe a longitudinal crack in an inner ply, something we have not observed from cold cycling. In this case delamination occurred not only in outer plies but also in an inner ply.

Imaging allowed us to observe damage induced from hot cycling. We observed that delamination occurred in both outer and inner plies; this could be seen from the propagation of longitudinal cracks from the outer to the inner plies and no transversal cracks were observed during the various tests and analyses carried out.

7. Conclusions

Carbon fiber reinforced cyanate ester composite laminates were subjected to flexural stresses and extreme thermal cycles to qualitatively assess damage using imaging, and for a quantitative measure of damage using the slope of unloading segments. Their microcracking behavior and mechanical performance were analyzed using in-situ micromechanical testing as well as

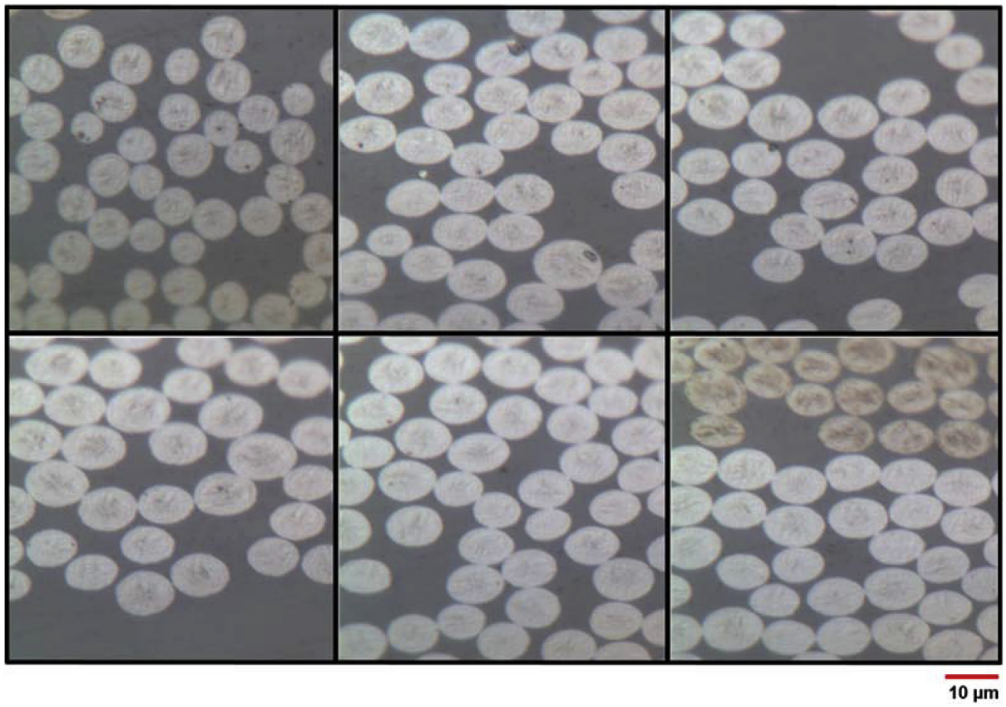

Fig. 9. Images taken from six different locations on the sample after 9 thermal cycles from −70 °C to 120 °C with DMA.

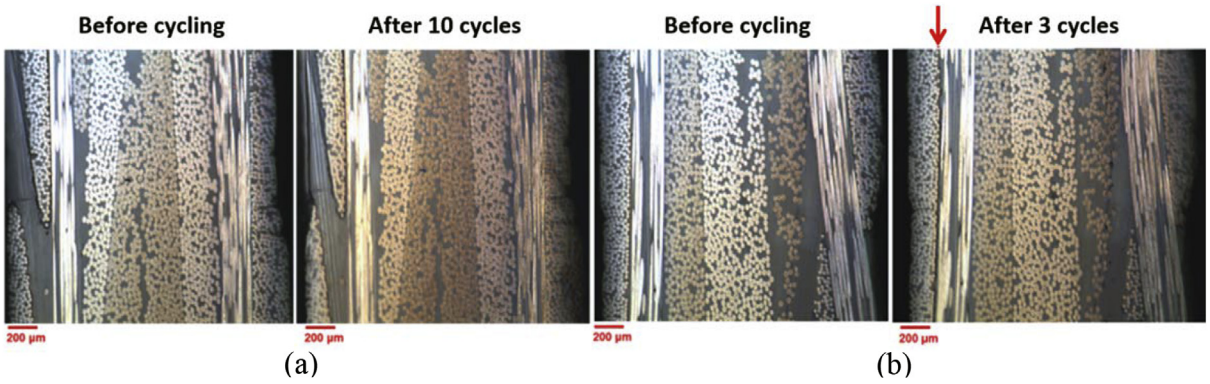

Fig. 10. a) Images taken before and after 10 cold cycles b) Images taken before and after 3 cold cycles.

thermomechanical and dynamic mechanical analyses techniques. The prominent results from this study are as follows:

- ❖ External mechanical loading induces damage in the material and the exact amount of damage can be assessed using a simple, non-destructive three point bending test. Such test demonstrated that the damage mechanism consist of microbuckling on the outer ply of the laminate, on the compression side, followed by delamination propagating on the inner plies of the material which eventually leads to its failure.
- ❖ Thermal cycling performed between 20 °C and −120 °C using DMA demonstrate no apparent damage on the material after eight cold cycles. Damage was assessed by monitoring the modulus during the tests and by taking before and after cycling images. Modulus values remained constant throughout the entire test and imaging showed no presence of microcracks which means that no damage was induced by such thermal cycling and therefore, no change in mechanical properties could be recorded.
- ❖ Extreme thermal cycling using a "fast dipping" method induced microcracking in the material in the form of longitudinal cracks causing delamination. Cold cycling was performed between 20 °C and −210 °C dipping quickly the material in liquid nitrogen and hot cycling between 20 °C and 100 °C dipping quickly the material in boiling water. Imaging before and after each cycle demonstrate the presence of damage in early cycles until completion of ten cycles. Mechanical testing in three point bending was carried out before and after five cycles on a cold cycled sample demonstrating almost 50% reduction in modulus after only five extreme cycles.

Fig. 11. a) Images taken before and after one and 10 hot cycles and b) Images taken before and after five and eight hot cycles.

Acknowledgments

The authors would like to thank CRIAQ and NSERC for their contribution to the funding of this project. J.A is also grateful to Professor Pascal Hubert for letting her use the TMA and DMA instruments.

References

[1] Marieta C, Schulz E, Irusta L, Gabilondo N, Tercjak A, Mondragon I. Evaluation of fiber surface treatment and toughening of thermoset matrix on the interfacial behaviour of carbon fiber-reinforced cyanate matrix composites. Compos Sci Technol 2005;65(14):2189–97.
[2] Paillous A, Pailler C. Degradation of multiply polymer-matrix composites induced by space environment. Composites 1994;25(4):287–95.
[3] Bechel VT, Fredin MB, Donaldson SL, Kim RY, Camping JD. Effect of stacking sequence on micro-cracking in a cryogenically cycled carbon/Bismaleimide composite. Compos Part A Appl Sci Manuf 2003;34(7):663–72.
[4] Biernacki K, Szyszkowski W, Yannacopoulos S. An experimental study of large scale model composite materials under thermal fatigue. Compos Part A Appl Sci Manuf 1999;30(8):1027–34.
[5] Choi J, Tamma KK. Woven fabric composites—Part I: predictions of homogenized elastic properties and micromechanical damage analysis. Int J Numer Methods Eng 2001;50(10):2285–98.
[6] Kim HS, Zhang J. Fatigue damage and life prediction of glass/vinyl ester composites. J Reinf Plastics Compos 2001;20(10):834–48.
[7] Marieta C, Schulz E, Mondragon I. Characterization of interfacial behaviour in carbon-fibre/cyanate composites. Compos Sci Technol 2002;62(2):299–309.
[8] Timmerman JF, Hayes BS, Seferis JC. Cure temperature effects on cryogenic microcracking of polymeric composite materials. Polym Compos 2003;24(1):132–9.
[9] Timmerman JF, Seferis JC. Predictive modeling of microcracking in carbon-fiber/epoxy composites at cryogenic temperatures. J Appl Polym Sci 2004;91(2):1104–10.
[10] Abdelal GF, Abuelfoutouh N, Hamdy A, Atef A. Thermal fatigue analysis of small-satellite structure. Int J Mech Mater Des 2006;3(2):145–59.
[11] Ahlborn K. Durability of carbon fibre reinforced plastics with thermoplastic matrices under cyclic mechanical and cyclic thermal loads at cryogenic temperatures. Cryogenics 1991;31(4):257–60.
[12] Han J-H, Kim C-G. Low earth orbit space environment simulation and its effects on graphite/epoxy composites. Compos Struct 2006;72(2):218–26.
[13] Iannucci L. Woven composite design for extreme events using a damage mechanics methodology. Proc Institution Mech Eng Part L J Mater Des Appl 2000;214(2):99–111.
[14] Issoupov V. Predictive model for microcracking and mechanical properties of polymer-matrix composite materials for space applications. Eur Space Agency, Special Publ ESA Sp 2003:407–12. 540.
[15] Kim RY, Crasto AS, Schoeppner GA. Dimensional stability of composite in a space thermal environment. Compos Sci Technol 2000;60(12–13):2601–8.
[16] Lafarie-Frenot MC. Damage mechanisms induced by cyclic ply-stresses in carbon–epoxy laminates: environmental effects. Int J Fatigue 2006;28(10):1202–16.
[17] Park CH, McManus HL. Thermally induced damage in composite laminates: predictive methodology and experimental investigation. Compos Sci Technol 1996;56(10):1209–19.
[18] Rouquie S, Lafarie-Frenot MC, Cinquin J, Colombaro AM. Thermal cycling of carbon/epoxy laminates in neutral and oxidative environments. Compos Sci Technol 2005;65(3–4):403–9.
[19] Schubbe JJ, Mucciardi AN. Investigation of bulk damage progression and inspection for GFRP laminate properties. J Mater Eng Perform 2012;21(7):1275–82.
[20] Shimokawa T, Katoh H, Hamaguchi Y, Sanbongi S, Mizuno H, Nakamura H, et al. Effect of thermal cycling on microcracking and strength degradation of high-temperature polymer composite materials for use in next-generation SST structures. J Compos Mater 2002;36(7):885–95.
[21] Bechel VT, Kim RY. Damage trends in cryogenically cycled carbon/polymer composites. Compos Sci Technol 2004;64(12):1773–84.
[22] He Y, Li Q, Kuila T, Kim NH, Jiang T, Lau K, et al. Micro-crack behavior of carbon fiber reinforced thermoplastic modified epoxy composites for cryogenic applications. Compos Part B Eng 2013;44(1):533–9.
[23] Lafarie-Frenot MC, Rouquie S. Influence of oxidative environments on damage in C/epoxy laminates subjected to thermal cycling. Compos Sci Technol 2004;64(10–11):1725–35.
[24] Lafarie-Frenot MC, Rouquié S, Ho NQ, Bellenger V. Comparison of damage development in C/epoxy laminates during isothermal ageing or thermal cycling. Compos Part A Appl Sci Manuf 2006;37(4):662–71.
[25] Bonora N, La Barbera A, Marchetti M. Experimental verification and theoretical simulation of fracture behaviours of composite materials. Compos Struct 1993;23(2):87–97.
[26] Rivera J, Karbhari VM. Cold-temperature and simultaneous aqueous environment related degradation of carbon/vinylester composites. Compos Part B Eng 2002;33(1):17–24.
[27] Savage G. Formula 1 composites engineering. Eng Fail Anal 2010;17(1):92–115.
[28] Lampman S. Characterization and failure analysis of plastics. ASM International; 2003.
[29] Karger-Kocsis J, Czigány T. Effects of interphase on the fracture and failure behavior of knitted fabric reinforced composites produced from commingled GF/PP yarn. Compos Part A Appl Sci Manuf 1998;29(9–10):1319–30.
[30] Colombo C, Vergani L. Experimental and numerical analysis of a bus component in composite material. Compos Struct 2010;92(7):1706–15.
[31] Kharoubi M. Study of the damage by acoustic emission of two laminate composites subjected to various levels of loading in three points bending. Mechanika 2007;5(67):48.
[32] Liu B, Lessard LB. Fatique and damage-tolerance analysis of composite laminates: stiffness loss, damage-modelling, and life prediction. Compos Sci Technol 1994;51(1):43–51.
[33] Plumtree A. Cyclic damage evolution in polymer matrix composites. Key Eng Mater 2010;417:1–4.
[34] Tompkins SS. Effects of thermal cycling on composite materials for space structures. In: Joint NASA/SDIO conference. Hampton, Virginia: NASA Langley Research Center; 1988.
[35] Zhang C, Binienda WK, Morscher GN, Martin RE, Kohlman LW. Experimental and FEM study of thermal cycling induced microcracking in carbon/epoxy triaxial braided composites. Compos Part A Appl Sci Manuf 2013;46(0):34–44.